Bayesian Approaches to Atmospheric Correction of Satellite Ocean-Color Imagery

Robert Frouin
Scripps Institution of Oceanography,
University of California San Diego, La Jolla, USA

(With contributions from Bruno Pelletier, University of Rennes, France and Lydwine Gross, CAPGEMINI, France.)

HysPIRI Aquatic Studies Group – Third Annual Forum
05 June 2015, NASA/GSFC, Greenbelt, Maryland

Ill-posed Nature of the inverse Problem

-The ocean color inverse problem (or atmospheric correction) is the retrieval of water reflectance from TOA reflectance.

-Multiple combinations of atmospheric and oceanic parameters (or pre-images) yield the same TOA reflectance. This places the inverse problem in a probabilistic context.

$$\rho \approx \rho_a + \rho_w T_a$$

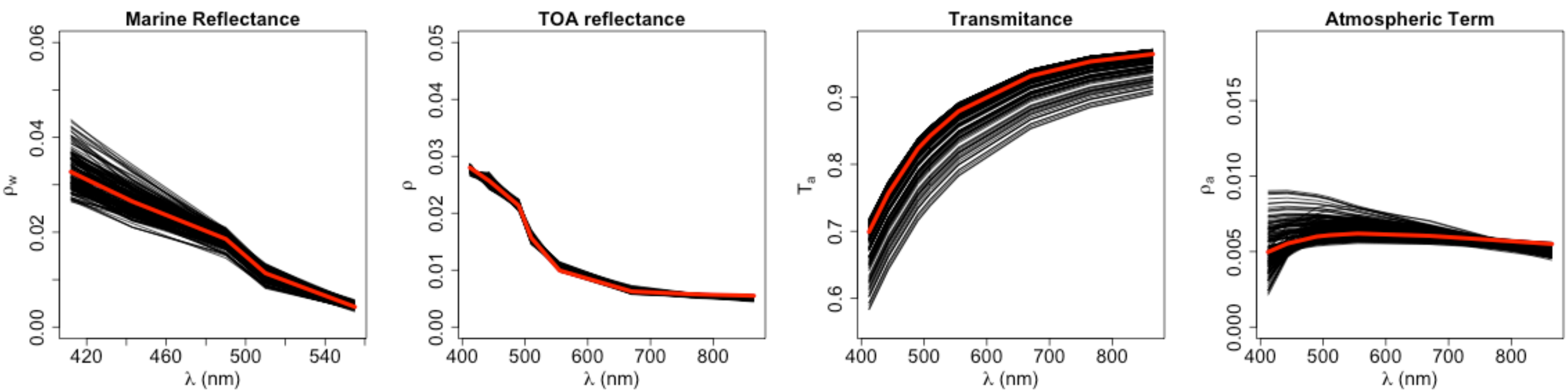

Example of pre-images. Actual values of ρ_w , ρ, T_a, and ρ_a are displayed in red, and the pre-images at a distance no more than δ = 0.001 are displayed in black. The search spaces for the pre-images include NOMAD and AERONET-OC data sets and maritime, continental, and urban aerosols in various proportions and amount.

Classic Atmospheric Correction Scheme

-The perturbing signal (aerosol reflectance) is sought within a sub-ensemble of possible solutions, selected conveniently to relate univocally spectral dependence of TOA signal in the NIR and/or SWIR (where the ocean may be considered black) to aerosol model.

-The sub-ensemble may be based on theoretical considerations, on statistics of observed aerosol models (e.g., from AERONET), but there is no guaranty that the obtained solution is the actual one.

-The aerosol model cannot be determined from the spectral dependence of the TOA signal in the NIR/SWIR. No sensitivity to aerosol absorption. Information about aerosol altitude is needed.

-Consequently, very strict masks are applied to the data, typically 15% daily coverage, and scheme basically works when/where aerosol amount is low (fortunately over most of the ocean).

-No uncertainties are associated to the retrievals. Accuracy is evaluated using too few match-up data sets.

-Advantage: No assumption is made about water reflectance.

Bayesian Methodology

-The forward model is written as: $\rho = \phi(\rho_w, x_a) + \varepsilon$, where ρ is the TOA reflectance, ρ_w is the water reflectance, x_a denote the atmospheric parameters, and ε is a random noise.

-In the Bayesian approach to inverse problems, ρ_w and x_a are treated as random variables. This defines a probabilistic model, where any vector of measurements y^{obs} is considered a realization of the random vector y.

-The probabilistic model is specified by the forward model together with the distributions of ε and of (ρ_w, x_a). The distribution of (ρ_w, x_a), called the prior distribution, describes in a probabilistic manner the prior knowledge one may have about ρ_w and x_a before the acquisition of the data.

Bayesian Methodology (cont.)

-The Bayesian solution of the inverse problem of retrieving (ρ_w, x_a) from y is defined as the conditional distribution $P[(\rho_w, x_a)/y]$. It is called the posterior distribution. Hence, given the observation y^{obs}, the solution is expressed as the probability measure $P[(\rho_w, x_a)/y = y^{obs}]$.

-One is generally interested in certain relevant characteristics of the posterior distribution: its mean, which gives an estimate of the parameters to retrieve (ρ_w and x_a), and its covariance, which provides an accompanying measure of uncertainty.

-One may also compute a p-value, i.e., the probability that y takes a value at least as extreme as y^{obs}. Since the whole procedure consists of inverting a forward model (a component of which is a RT model), the p-value allows one to detect situations for which the forward model is unlikely to explain the data.

Connection with the Classical Scheme

-Consider the conditional expectation $E[\rho_w/\rho]$. Since $E[\rho_w/\rho]= E[E[\rho_w/\rho, x_a]/\rho]$, we see that $E[\rho_w/\rho, x_a]$ can be modeled first, and then averaged conditionally on ρ in a second time.

-This corresponds to inverting ρ assuming that the atmosphere is in the state x_a, and then averaging the results according to the distribution of x_a given ρ.

-So, compared with the classical approach, instead of picking an aerosol model and then inverting ρ assuming the atmosphere is in the state x_a, the Bayesian methodology amounts to placing a probability distribution on x_a, depending on ρ, inverting ρ for each x_a, and then averaging the results accordingly.

Inverse Modeling in Practice
(Frouin and Pelletier, RSE 159, 2015)

1) Specify prior distributions P_w and P_a

Assumed uniform for all parameters except aerosol optical thickness (log-normal); ρ_w from measurements, i.e., NOMAD and AERONET-OC datasets; aerosol parameters from WMO maritime, continental, and urban models.

2) Estimate P_ε

By comparing TOA values from selected imagery with forward model predictions.

3) Approximate numerically expectation and covariance, and p-value

By using models constructed on a partition of the space of TOA reflectance. These models allow one to keep the execution time small, i.e., suitable for use on an operational basis.

Theoretical Performance for SeaWiFS

a) Average Errors

Geometry-averaged statistics: ρ_w bias and standard deviation per channel, averaged over all the geophysical conditions and observation geometries.

Wavelength (nm)	412	443	490	510	555	670
Average Bias	1.81E-09	-8.06E-10	3.48E-09	3.06E-10	-1.08E-08	-4.66E-09
Average Standard Deviation	0.004321	0.003564	0.003220	0.002936	0.002652	0.001145

b) Errors per viewing geometry

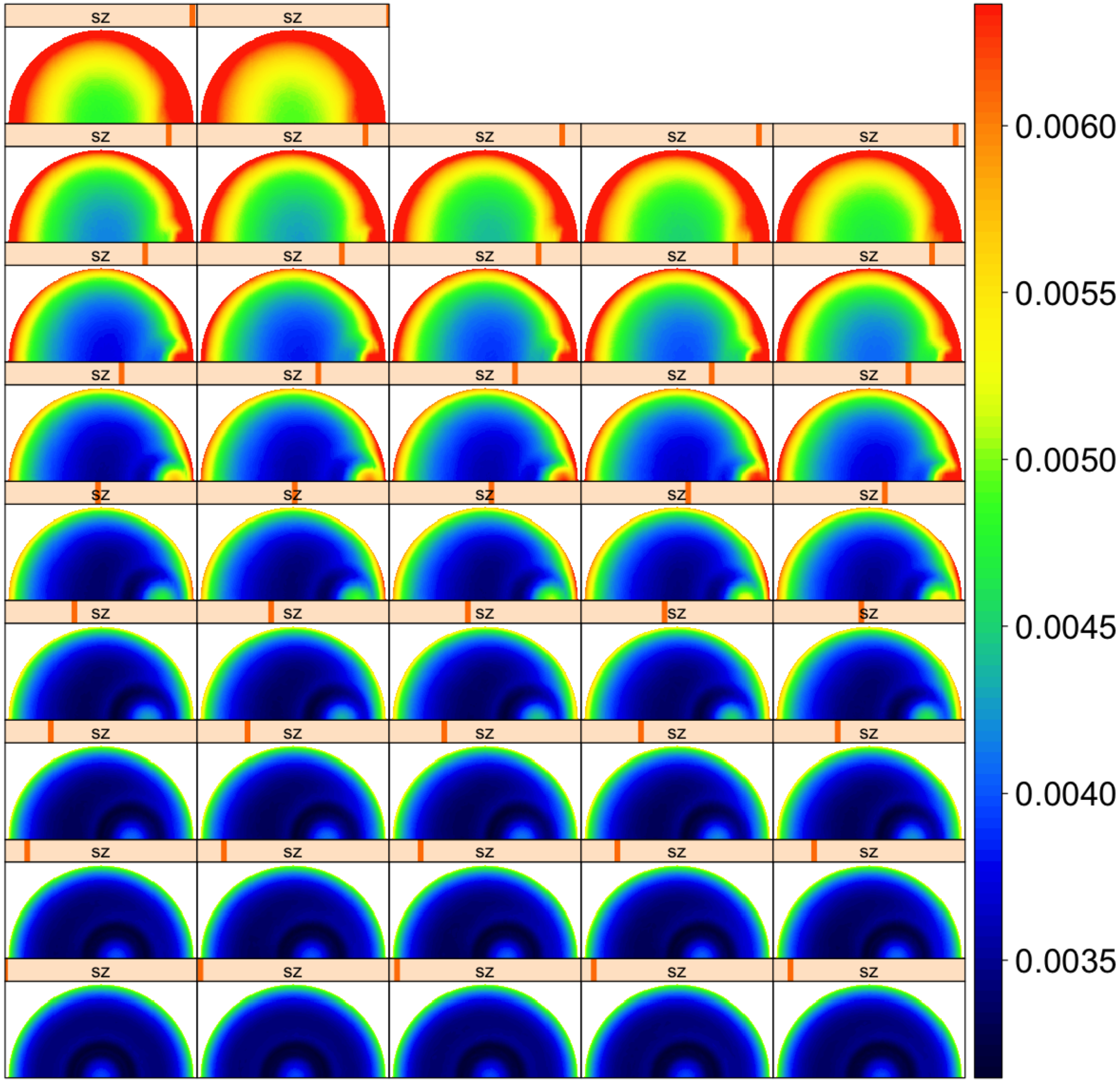

Standard deviation for each angular geometry at 412 nm. Each polar plot corresponds to a Sun zenith angle (SZ) in the range 0-76 deg. Radius depicts sine of view zenith angle from 0 to 76 deg.

c) Errors per aerosol optical thickness

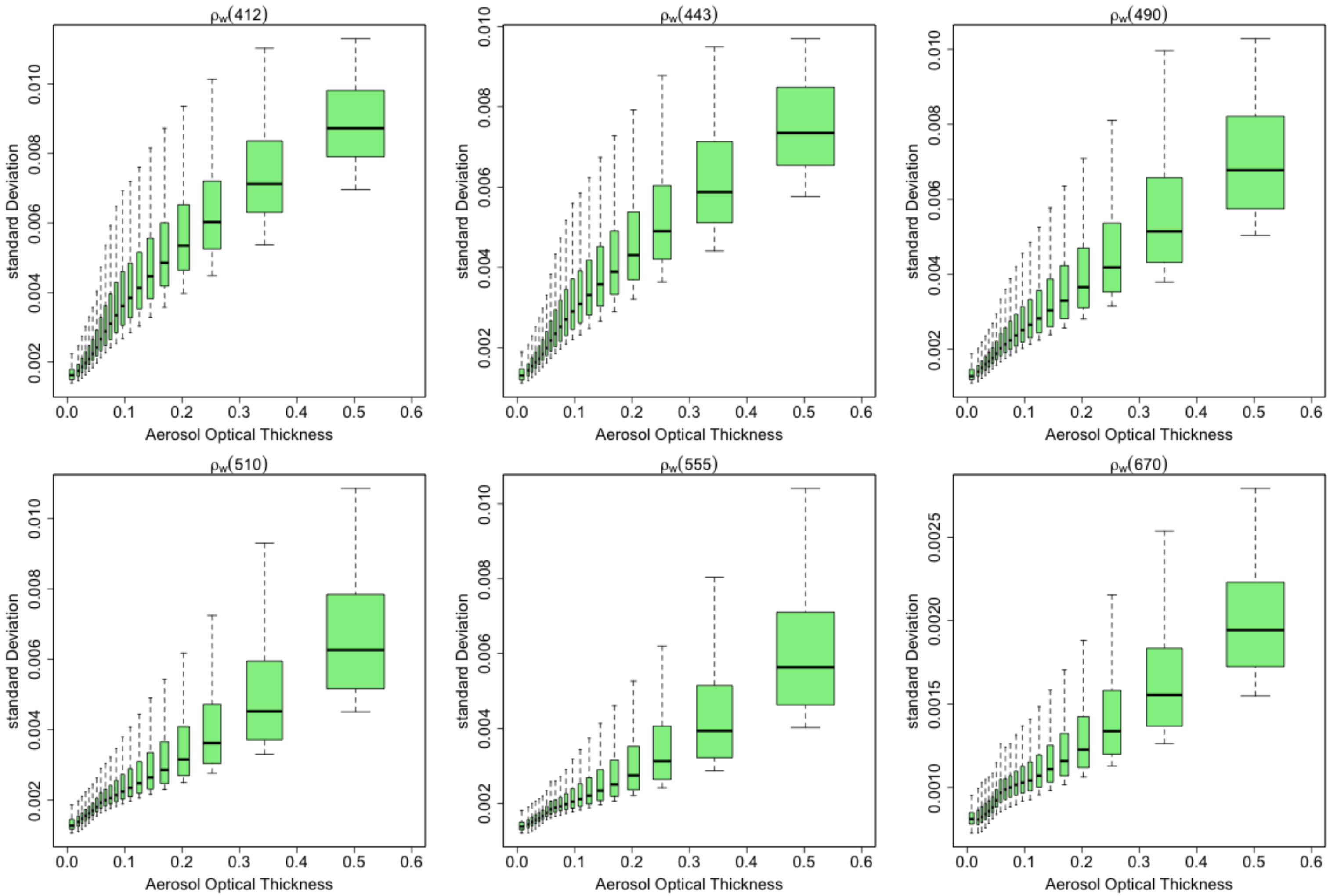

Standard deviation per spectral band aerosol optical thickness bin, with all the geometries.

d) Errors per aerosol type

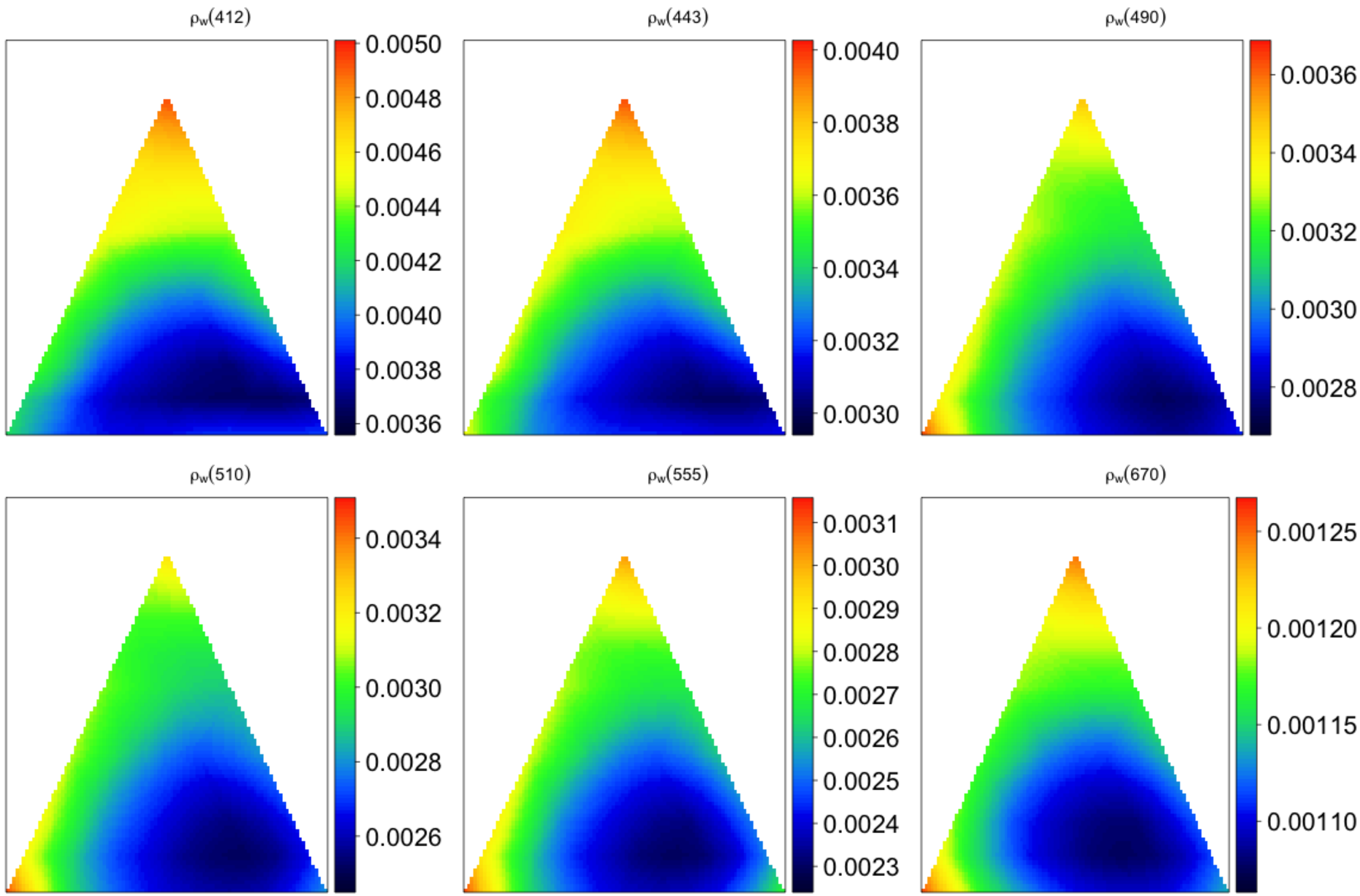

Standard deviation per spectral band, averaged all geometries, as a function of the aerosol type. Maritime aerosols: right corner of triangles, urban: top corner, and continental: left corner.

Evaluation against in Situ Measurements

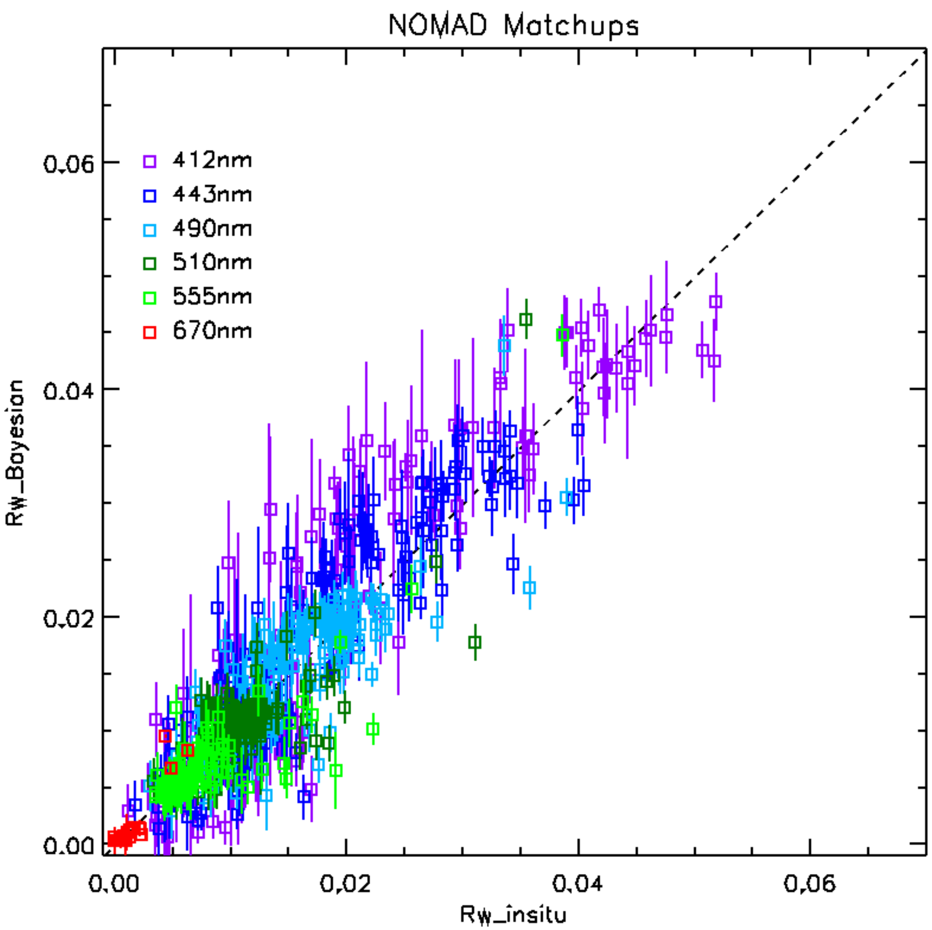

λ (nm)	R^2	Bias	RMSD	N
412	0.838	0.0016	0.0059	132
443	0.806	0.0009	0.0045	144
490	0.671	-0.0002	0.0034	144
510	0.587	-0.0005	0.0030	113
555	0.722	-0.0007	0.0026	129
670	0.820	<0.0001	0.0012	28
All	0.852	0.0002	0.0040	690

Comparison between marine reflectance estimated from SeaWiFS data using the Bayesian technique and measured in situ (NOMAD match-ups).

Application to SeaWiFS Imagery, South Africa, 02/14/1999

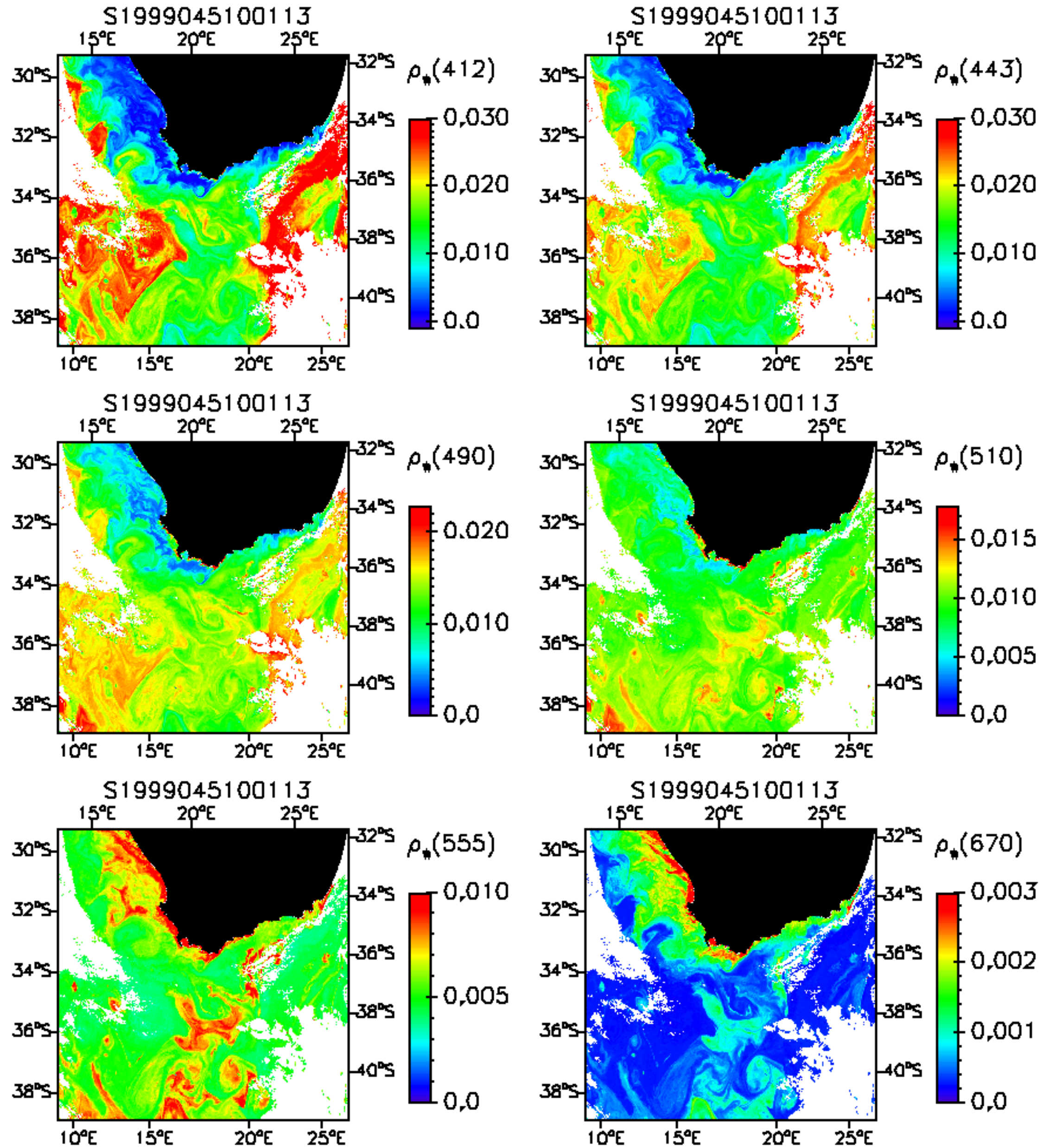

Estimated marine reflectance, Bayesian methodology.

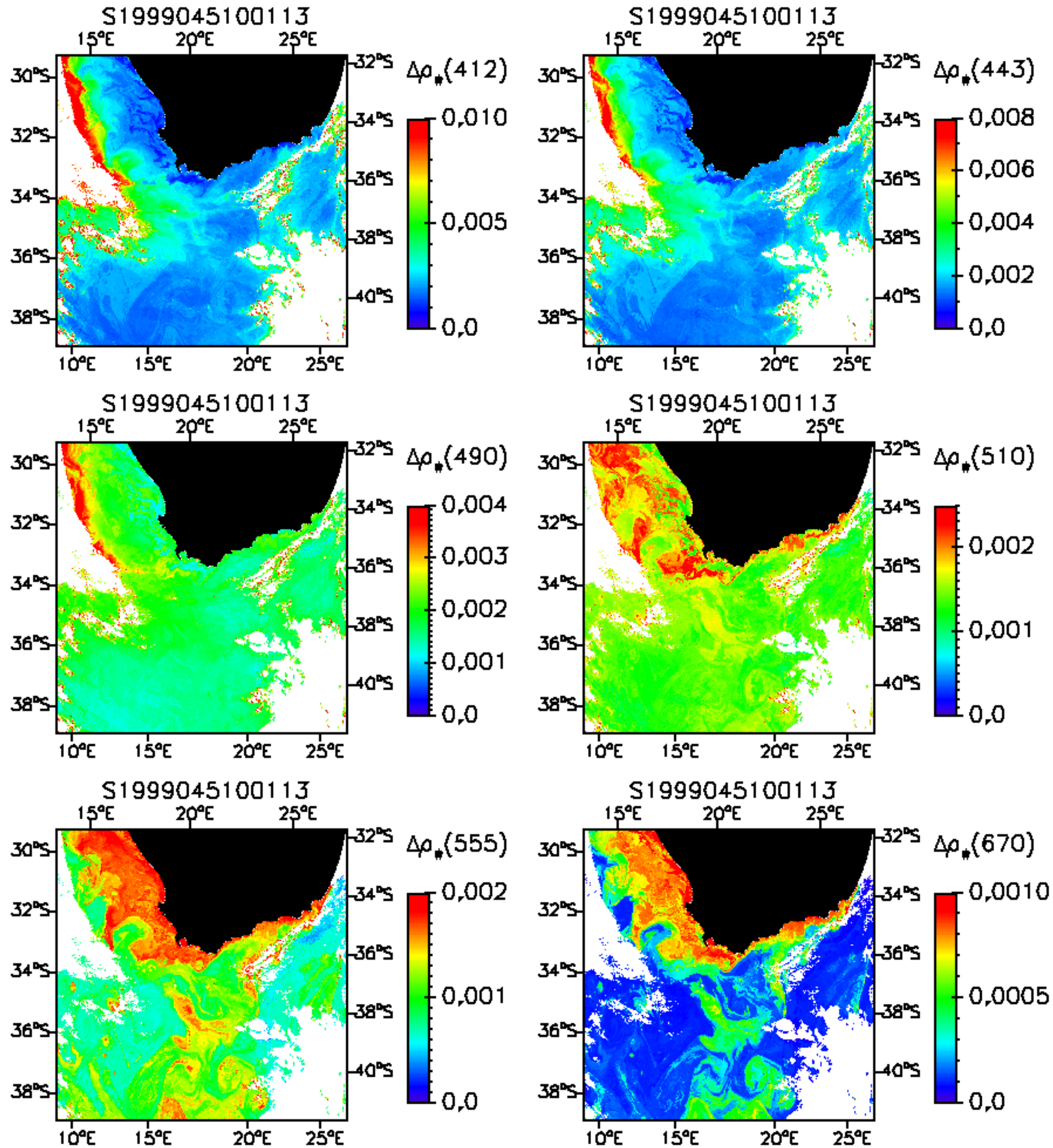

Estimated uncertainty on marine reflectance, Bayesian methodology.

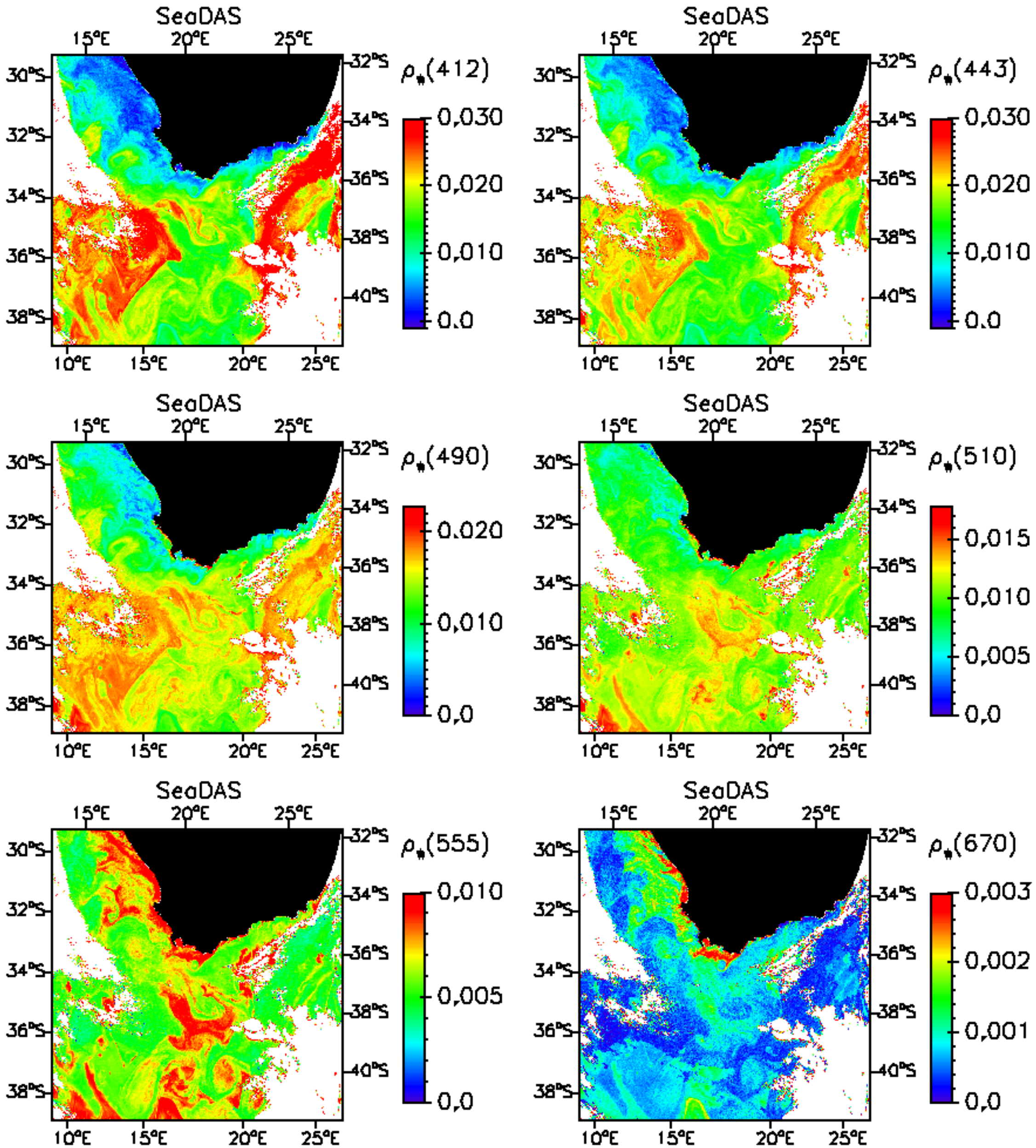

Estimated marine reflectance, SeaDAS algorithm.

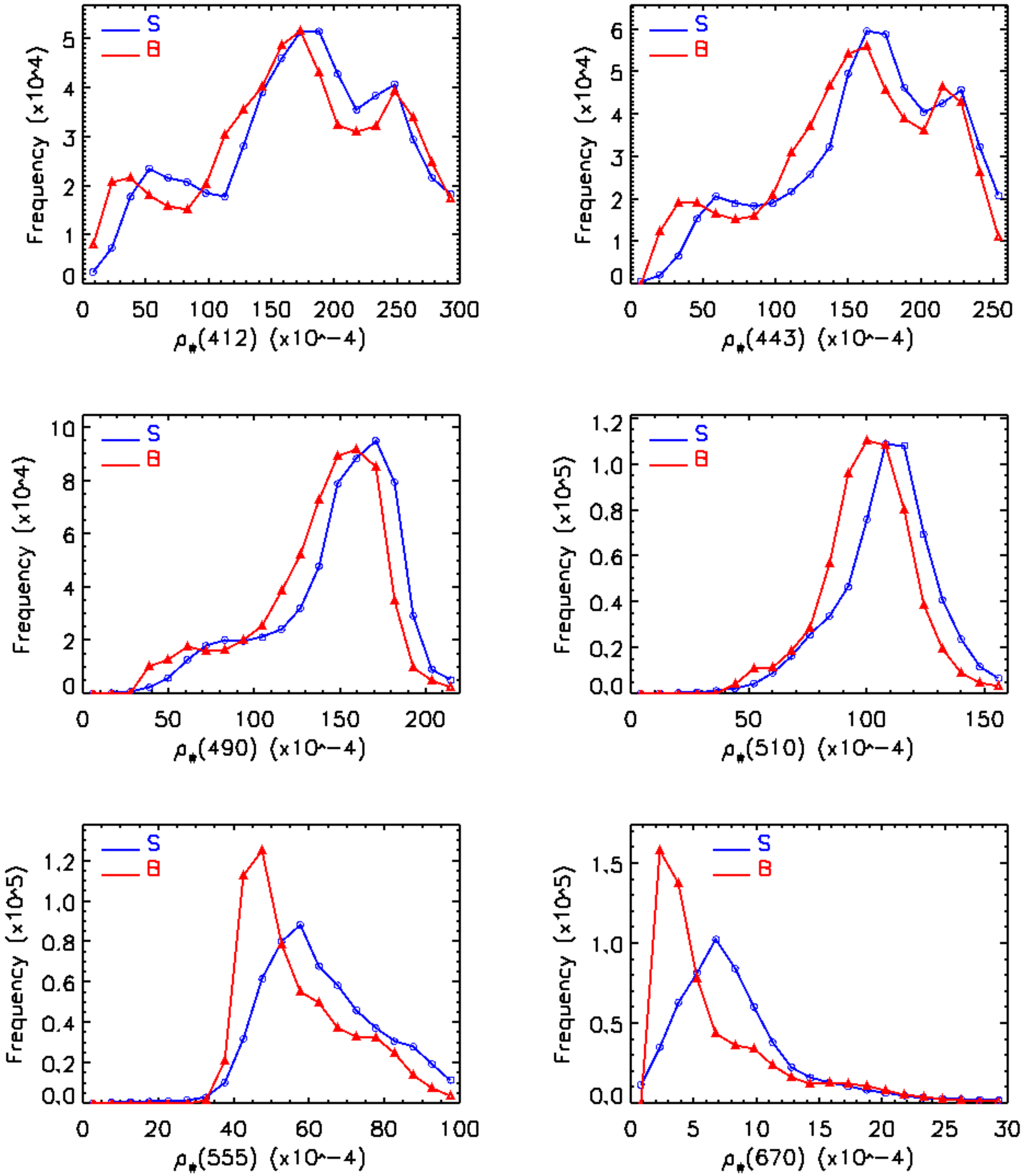

Histograms of valid marine reflectance estimates.

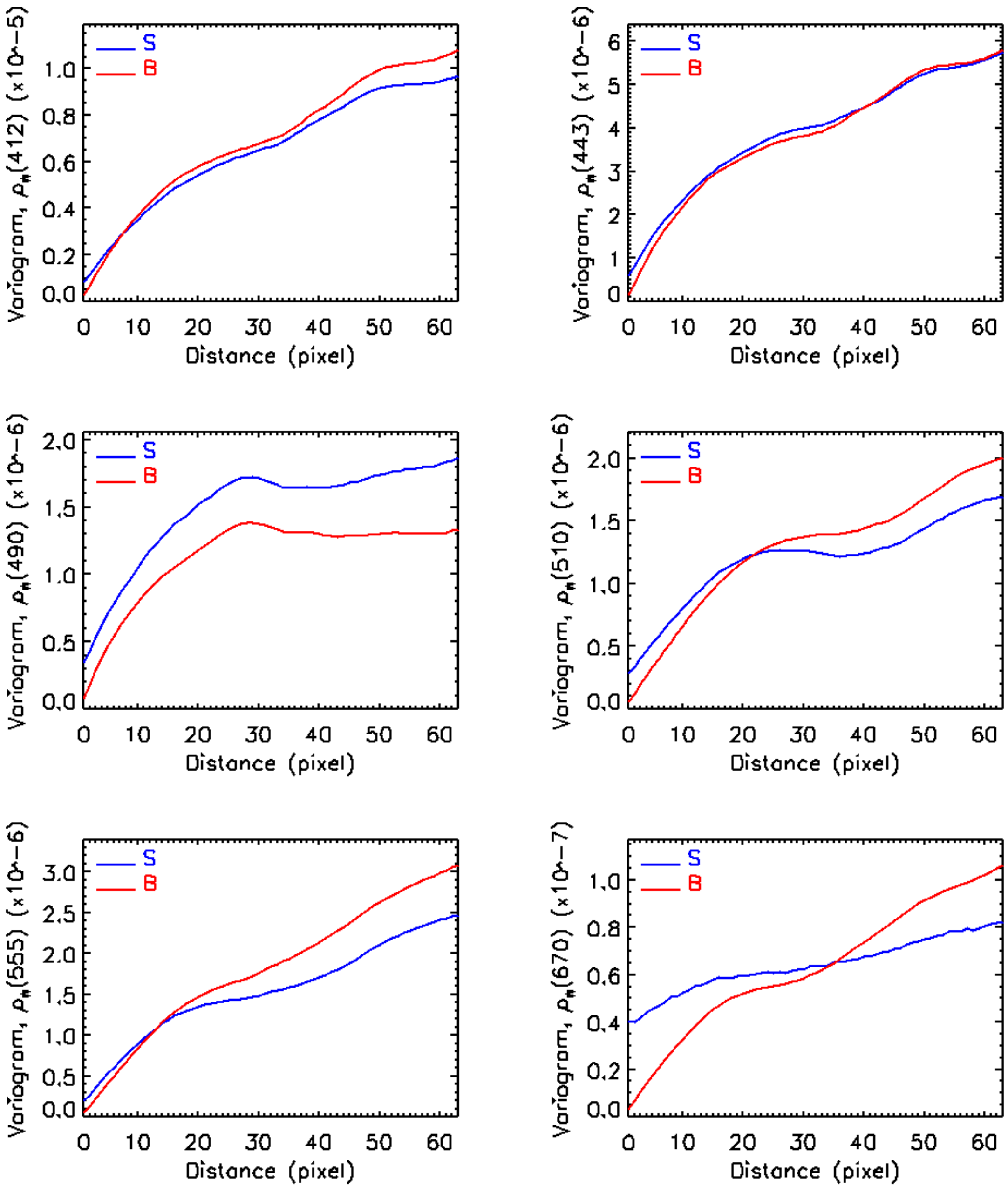

Variograms of valid marine reflectance estimates in selected area.

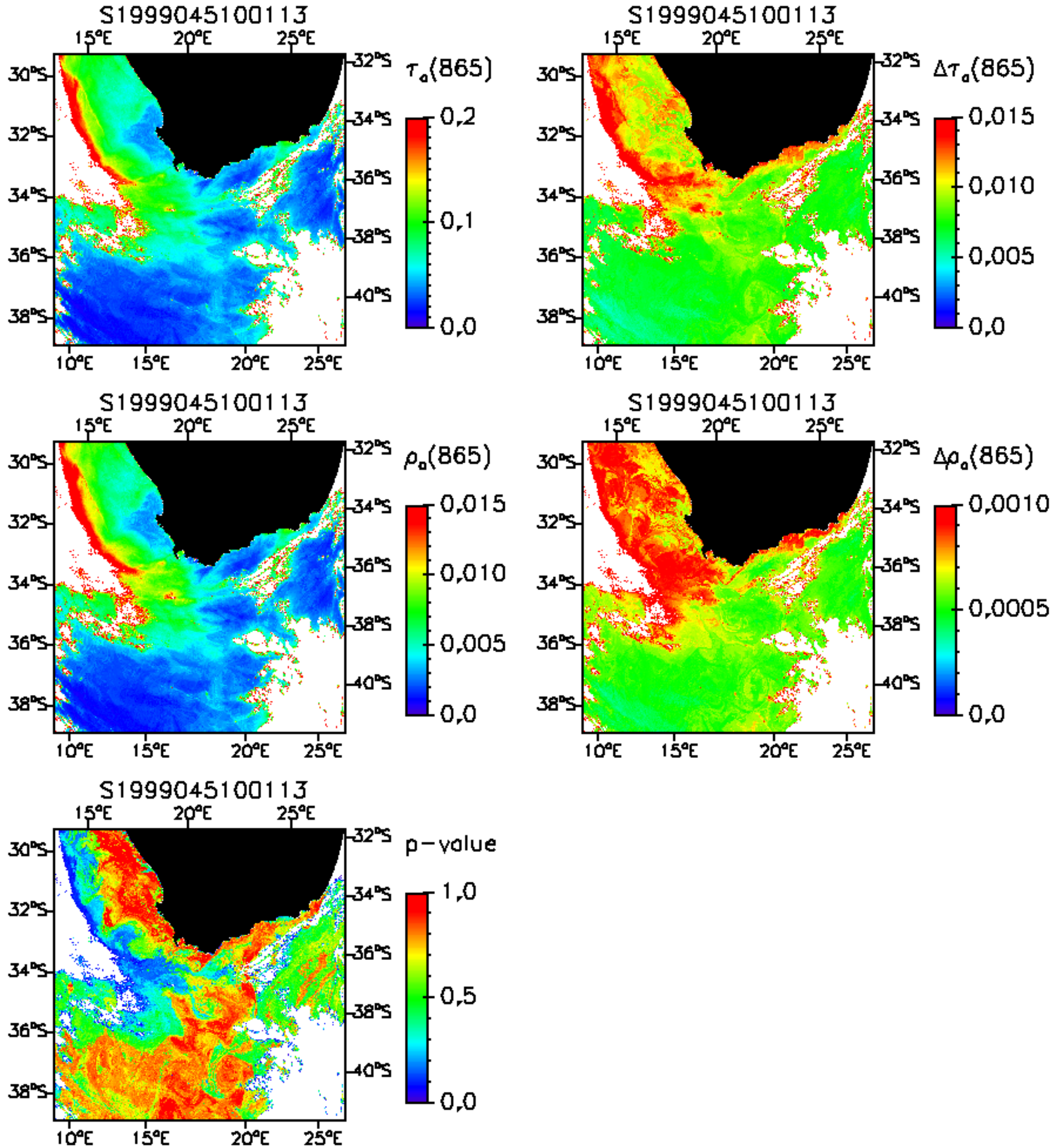

Estimated τ_a, ρ_a, and associated uncertainties, and p-value, Bayesian methodology.

Application to SeaWiFS Imagery, Other Regions

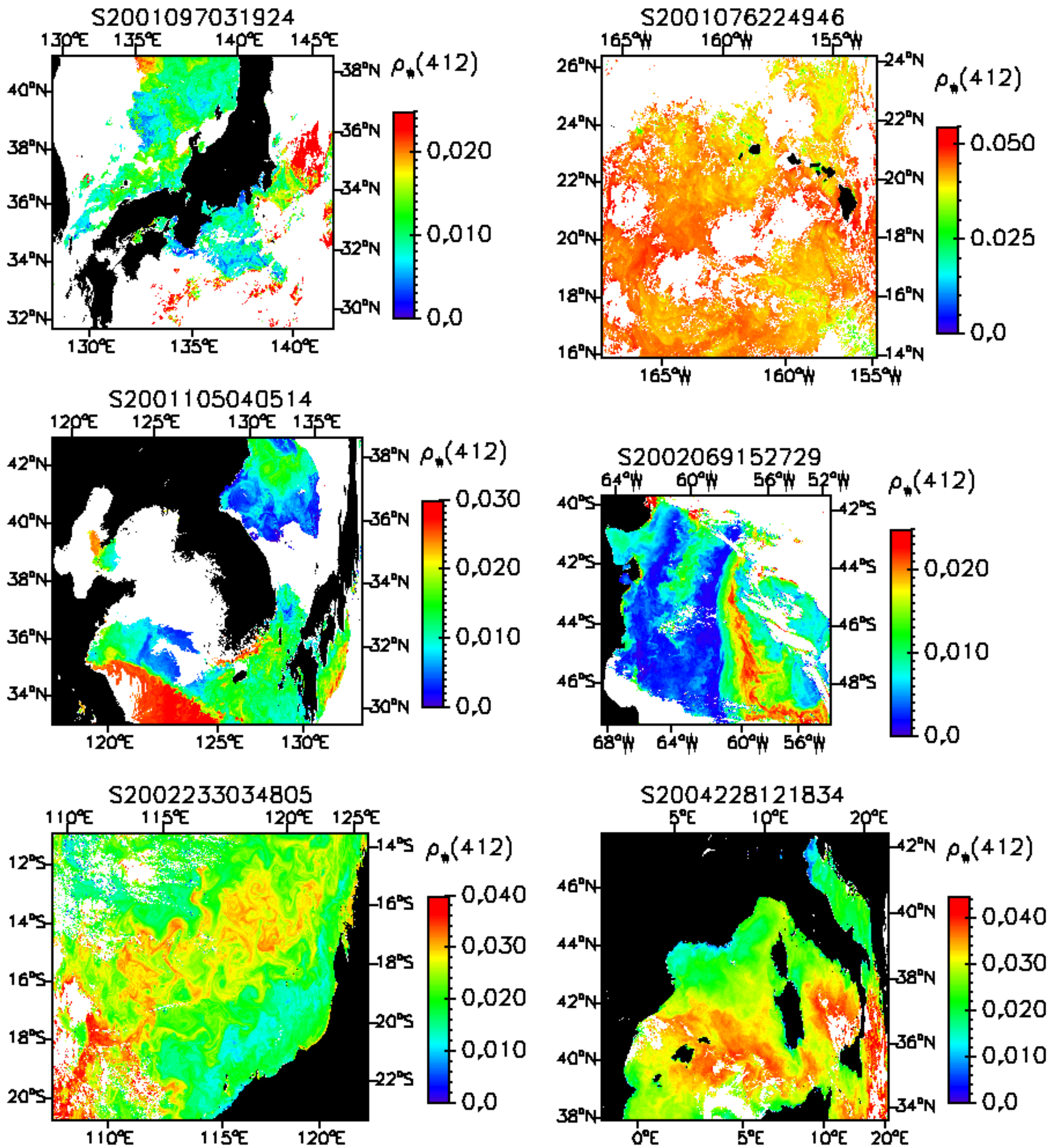

Marine reflectance imagery at 412 nm in various regions, Bayesian methodology.

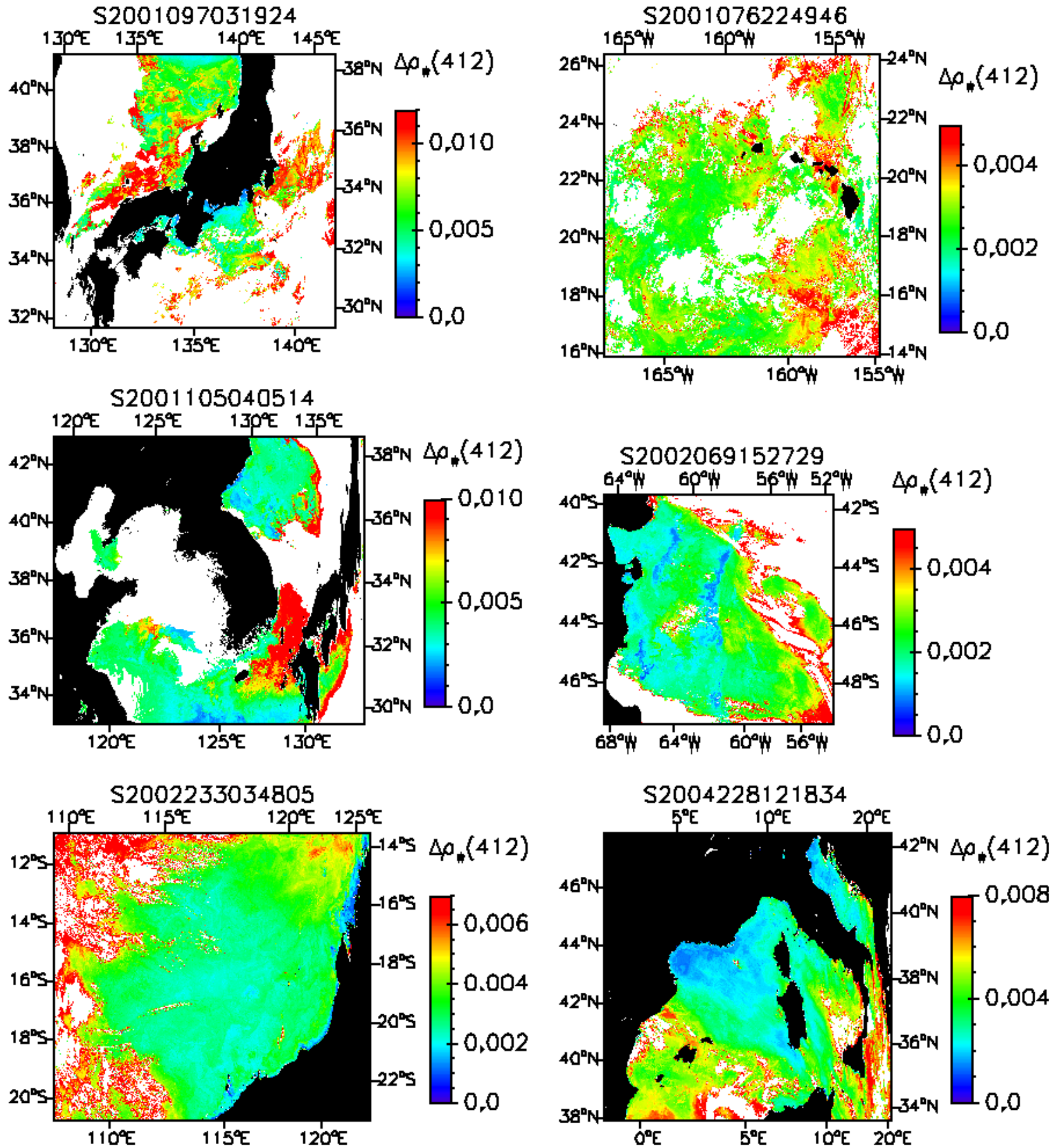

Uncertainty associated with marine reflectance retrievals at 412 nm.

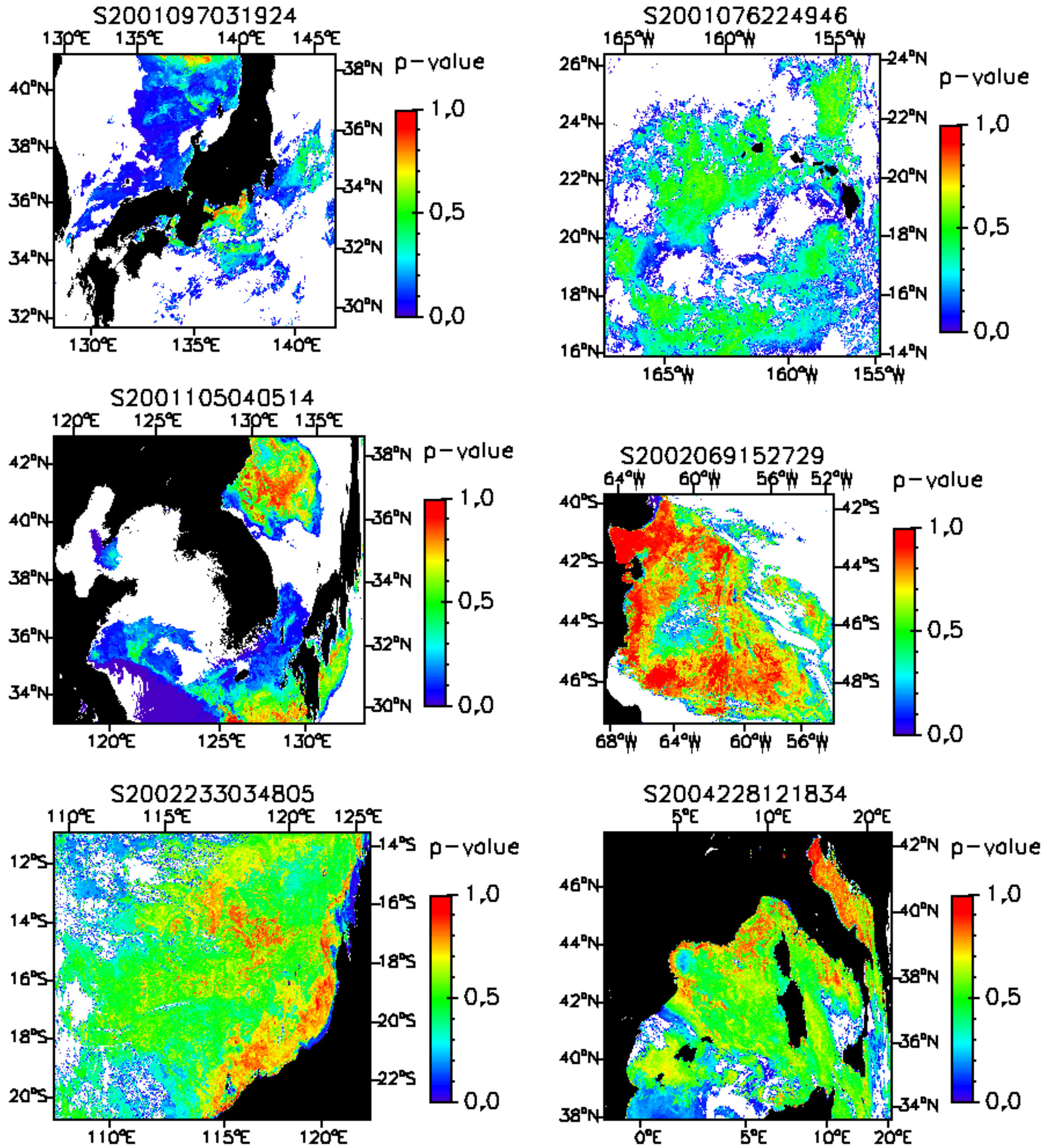

p-value (retrieval quality index) associated with marine reflectance estimates at 412 nm.

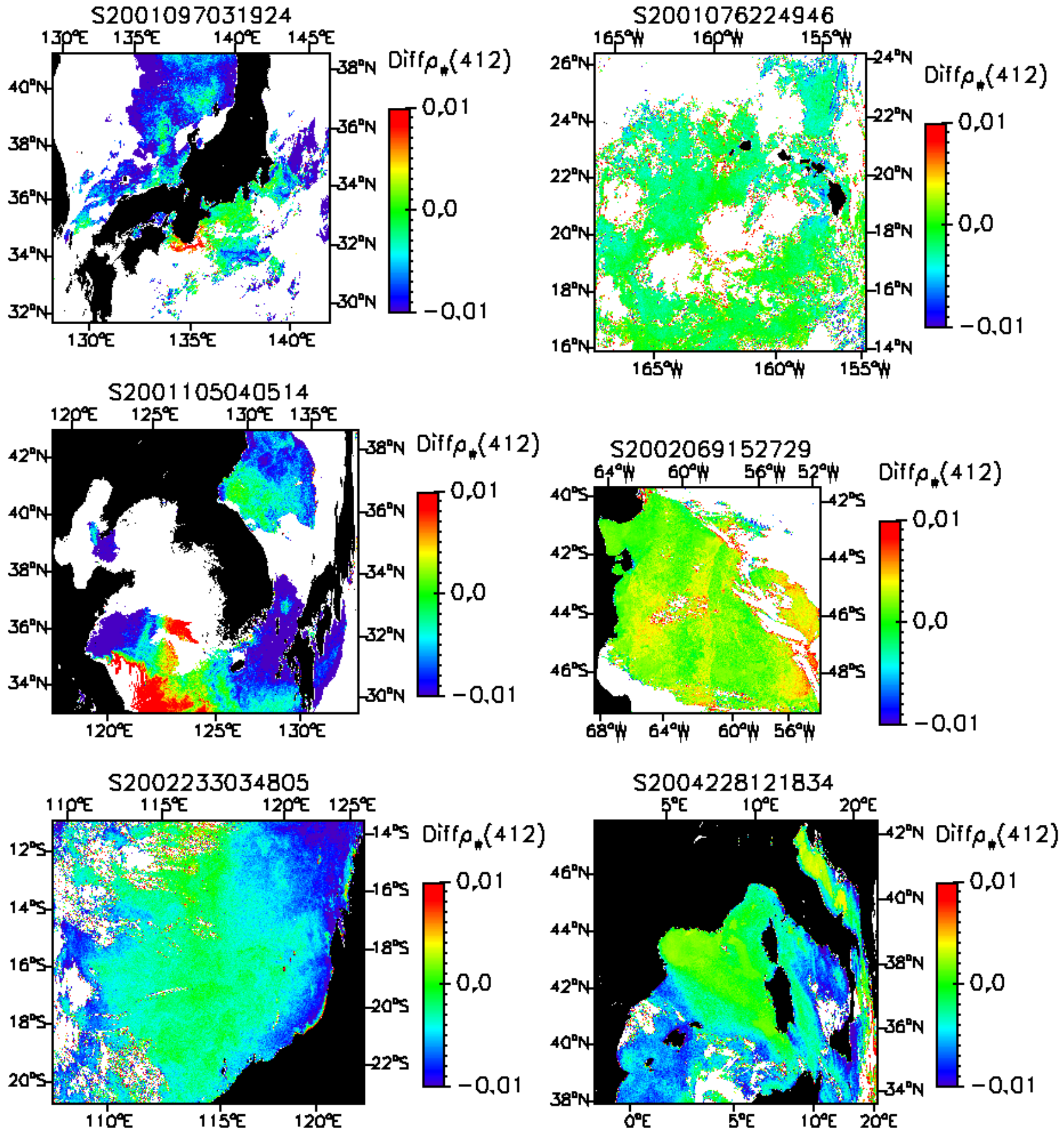

Differences between marine reflectance estimates at 412 nm from SeaDAS and the Bayesian methodology.

Neural Network with PCA
(Gross et al., SPIE 6680, 2007)

-TOA reflectance (after correction for molecular scattering effects) is decomposed in principal components.

-Components sensitive to the ocean signal are selected and combined to retrieve the principal components of marine reflectance, allowing reconstruction of the marine reflectance.

$$\rho_{\mathbf{p}} = \rho - \rho_{\mathbf{m}} = f(\rho_{\mathbf{w}})$$

$$\rho_{\mathbf{p}} = \sum_i c_{pi} \, \mathbf{e}_{\mathbf{p}i}$$

$$\rho_{\mathbf{w}} = \sum_j c_{wj} \mathbf{e}_{\mathbf{w}j}$$

$$c_{wj} = g_j(c_{pi})$$

-Functions g_j relating c_{pi} to c_{wj} approximated using multilayer perceptrons.

Correlation coefficients between the principal components of ρ_p, c_{pi}, and of ρ_w, c_{wj}; Empirical functions based on linear correlation matrix; Canonical correlation k between desired c_{wj} and the set of c_{pi} selected to calculate it.

Sensor	Linear correlation matrix														Empirical functions	k (%)
POLDER		cp1	cp2	cp3	cp4	cp5	cp6									
	cw1	5.8	-39.1	-77.6	-25.8	-10.6	0.6								cw1 = f(cp3, cp4, cp5)	90.2
	cw2	8.1	-10.8	24.3	-24.2	29.7	4.4								cw2 = g(cp3, cp4, cp5)	65.4
	cw3	0.6	6.1	10.2	-58.4	24.5	-2.1								cw3 = h(cp3, cp4, cp5)	42.1
SeaWiFS		cp1	cp2	cp3	cp4	cp5	cp6	cp7	cp8							
	cw1	2.1	23.6	-59.4	-64.4	14.6	-13.2	-15.5	-4.5						cw1 = f(cp3, cp4, cp5, cp6, cp7)	91.1
	cw2	10.8	7.0	36.7	-8.2	-27.5	-53.9	-57.3	-2.3						cw2 = g(cp3, cp4, cp5, cp6, cp7)	91.4
	cw3	5.9	-12.7	31.3	-48.0	-54.1	39.6	13.5	-6.3						cw3 = h(cp3, cp4, cp5, cp6, cp7)	89.2
MODIS		cp1	cp2	cp3	cp4	cp5	cp6	cp7	cp8	cp9						
	cw1	0.5	23.7	-63.0	-64.6	-3.3	-1.3	-6.6	-2.0	4.2					cw1 = f(cp3, cp4, cp7)	90.5
	cw2	11.0	8.2	35.7	-17.3	33.9	31.2	-60.9	-11.3	12.3					cw2 = g(cp3, cp4, cp5, cp6, cp7, cp8)	86.8
	cw3	5.9	-12.4	28.0	-30.5	57.5	-44.8	27.6	1.0	-14.3					cw3 = h(cp3, cp4, cp5, cp6, cp7)	88.3
MERIS		cp1	cp2	cp3	cp4	cp5	cp6	cp7	cp8	cp9	cp10	cp11	cp12	cp13		
	cw1	-7.4	2.2	-72.6	-41.6	-23.4	-1.4	-3.2	-2.9	-1.2	-0.8	0.8	-0.4	-0.1	cw1 = f(cp3, cp4, cp5)	86.6
	cw2	11.5	22.6	4.9	30.9	-9.0	-4.1	-18.9	0.0	-2.8	-3.0	-0.1	0.5	0.2	cw2 = g(cp3, cp4, cp5, cp6, cp7, cp9,cp10)	38.0
	cw3	-0.4	1.1	18.1	27.8	-35.6	-5.7	6.5	0.6	-1.3	0.3	0.8	-0.4	0.1	cw3 = h(cp3, cp4, cp5, cp6, cp7)	49.1

Application to POLDER Imagery, Black Sea

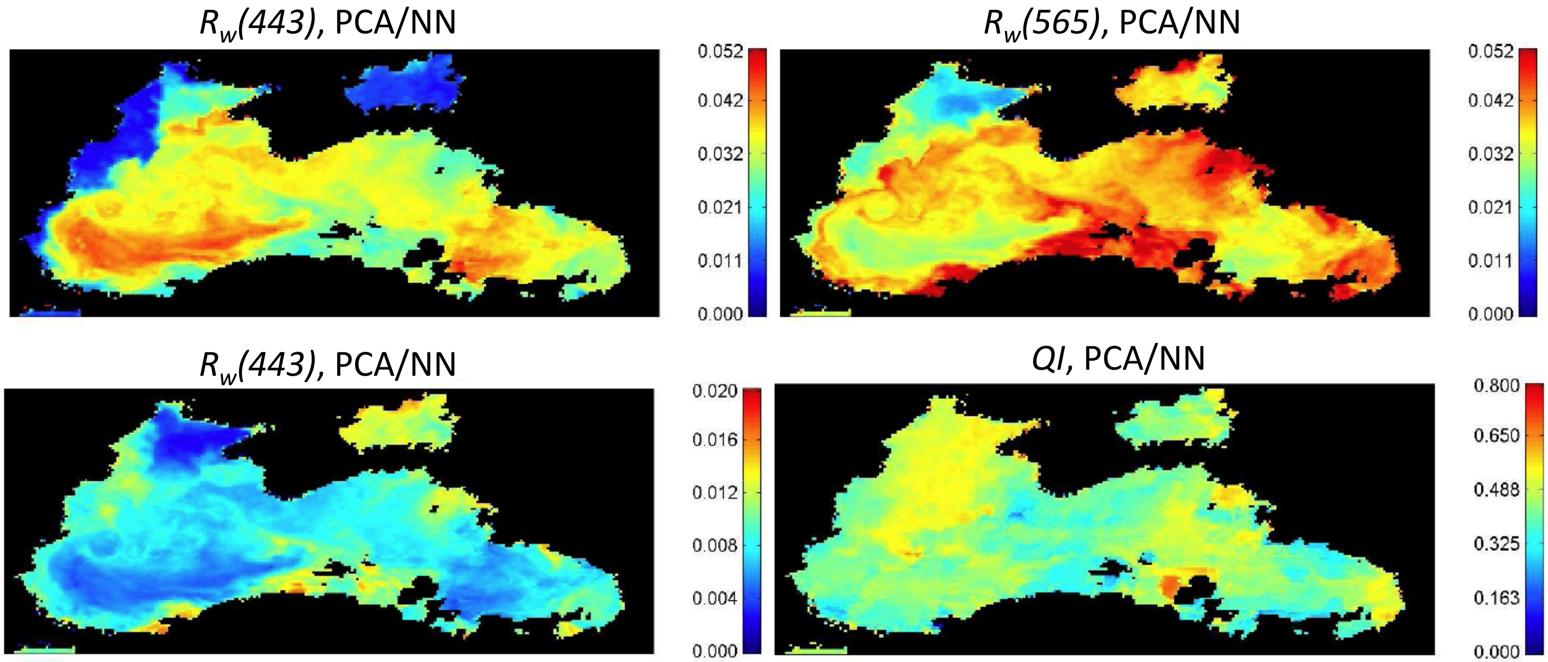

POLDER synthesis of marine reflectance for the first decade of June 2003, Black Sea, using the NN/PCA method. (Upper left) $R_w(443)$. (Upper right) $R_w(565)$. (Lower left) $R_w(670)$, not retrieved by the standard POLDER algorithm. (Lower right) QI. Note that QI is not correlated to detected features.

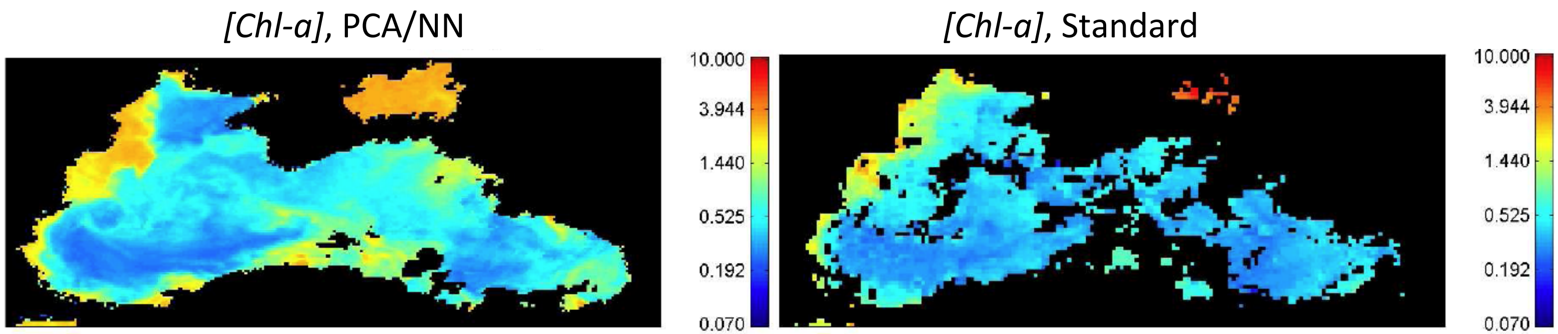

POLDER synthesis of of chlorophyll-a concentration for the first decade of June 2003, Black Sea. (Left) PCA/NN method. (Right) Standard POLDER algorithm.

Application to SeaWiFS Imagery, West Australia

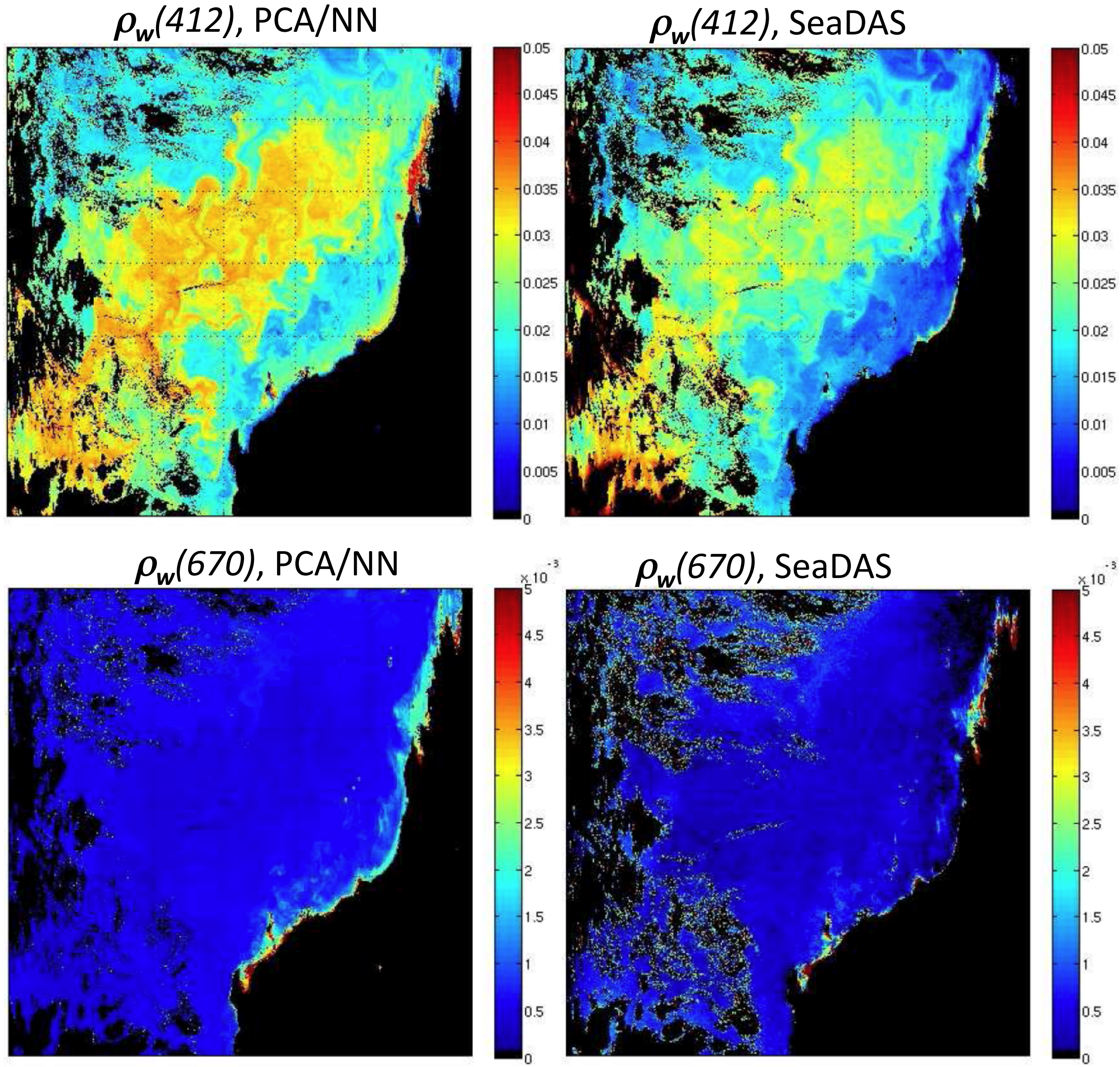

Marine reflectance retrieved using the PCA/NN method (left) and SeaDAS (right). NN reflectance is slightly higher in the blue. NN imagery is less noisy.

Application to MERIS, Northeast Atlantic

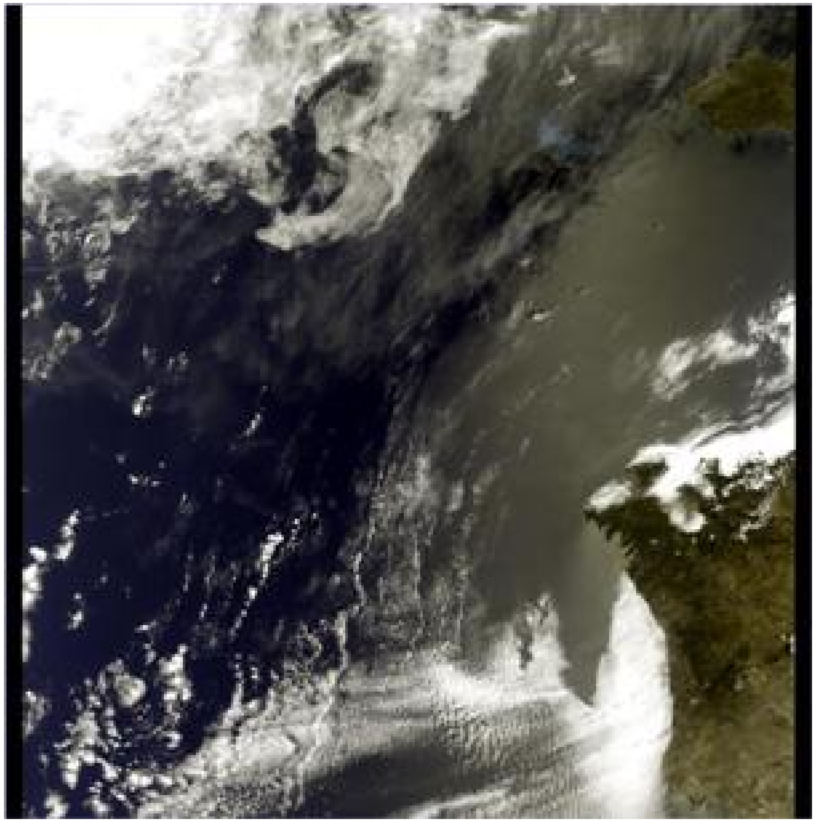

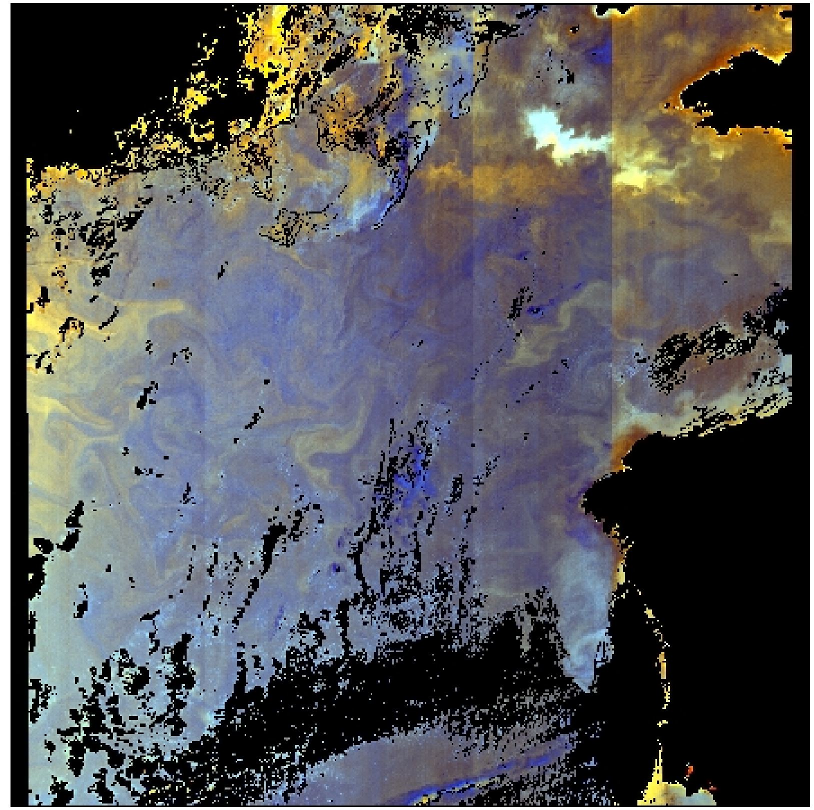

(Left) RGB composite of MERIS imagery off the coast of France and Portugal, 21 June 2005. (Right) RGB composite of marine reflectance retrieved by the PCA/NN algorithm. Marine reflectance is retrieved in the presence of thin clouds and sun glint.

Application to MERIS, Black Sea

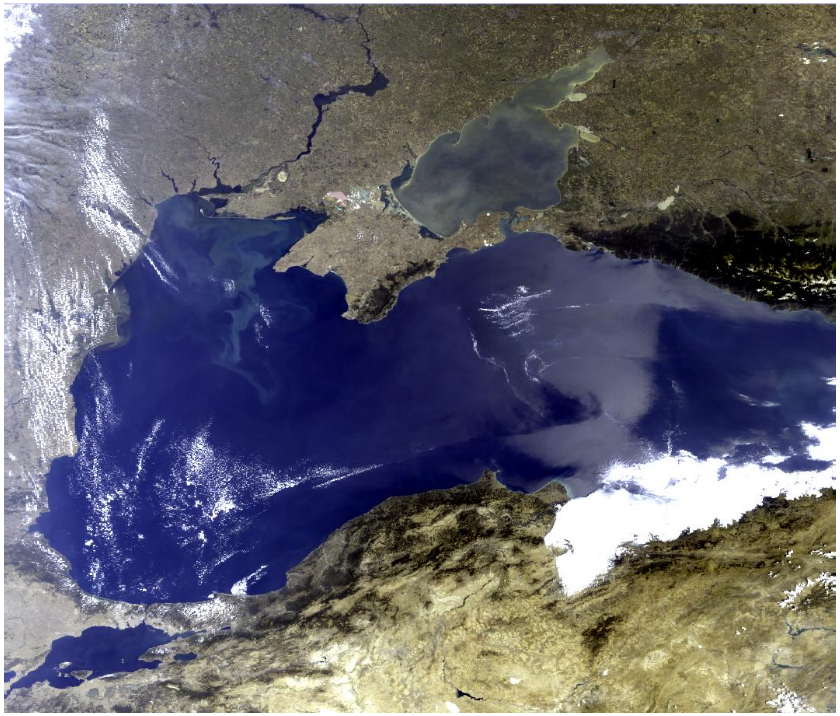

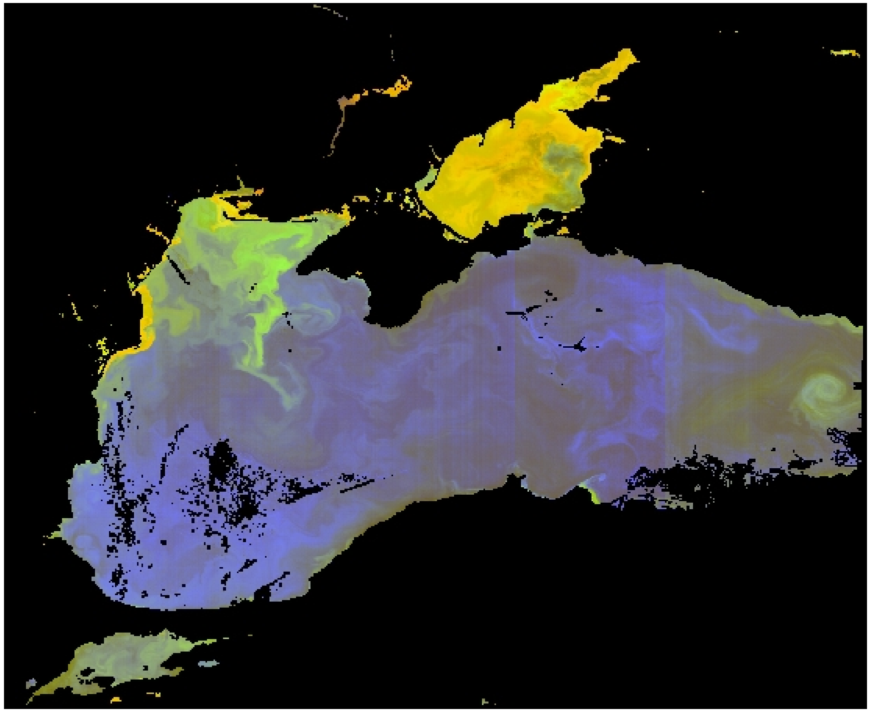

(Left) RGB composite of MERIS imagery of the Black Sea and Sea of Azov, 9 August 2008. (Right) RGB composite of marine reflectance retrieved by the PCA/NN algorithm. Marine reflectance is retrieved in the presence of thin clouds and sun glint.

Conclusions

Bayesian approaches are adapted to the ill-posed nature of the ocean color inverse problem. They constitute a valuable alternative to the classic atmospheric correction scheme.

-They allow the construction of reliable multi-dimensional confidence domains of the retrieved marine reflectance.

-They have the potential to provide accurate estimates in sun glint and thin cloud conditions, and absorbing aerosols, i.e., to increase substantially the daily coverage of ocean-color products.

-Regionalization of the inverse models is a natural development to improve retrieval accuracy, for example by including explicit knowledge of the space and time variability of atmospheric variables.